Biosensors and Bioelectronics 25 (2010) 2212–2217

Contents lists available at ScienceDirect

Biosensors and Bioelectronics

journal homepage: www.elsevier.com/locate/bios

Extracellular potentials recording in intact olfactory epithelium by microelectrode array for a bioelectronic nose

Qingjun Liu[a,b], Weiwei Ye[a], Lidan Xiao[a], Liping Du[a], Ning Hu[a], Ping Wang[a,b,*]

[a] Biosensor National Special Laboratory, Key Laboratory of Biomedical Engineering of Education Ministry, Department of Biomedical Engineering, Zhejiang University, Hangzhou 310027, PR China
[b] State Key Laboratory of Transducer Technology, Chinese Academy of Sciences, Shanghai 200050, PR China

ARTICLE INFO

Article history:
Received 4 January 2010
Received in revised form 11 February 2010
Accepted 23 February 2010
Available online 1 March 2010

Keywords:
Bioelectronic nose
Cell and tissue based biosensor
Olfactory epithelium
Microelectrode array (MEA)
Olfactory receptor neurons

ABSTRACT

Human beings and animals have sensitive olfactory systems that can sense and identify a variety of odors. The purpose of this study is to combine biological cells with micro-chips to establish a novel bioelectronic nose system for odor detection by electrophysiological sensing measurements of olfactory tissue. In our experiments, 36-channel microelectrode arrays (MEAs) with the diameter of 30 μm were fabricated on the glass substrate, and olfactory epithelium was stripped from rats and fixed on the surface of MEA. Electrophysiological activities of olfactory receptor neurons in intact epithelium were measured through the multi-channel recording system. The extracellular potentials of cell networks could be effectively analyzed by correlation analysis between different channels. After being stimulated by odorants, such as acetic acid and butanedione, the olfactory cells generate different firing modes. These firing characteristics can be derived by time-domain and frequency-domain analysis, and they were different from spontaneous potentials. The investigation of olfactory epithelium can provide more information of olfactory system for artificial olfaction biomimetic design.

© 2010 Elsevier B.V. All rights reserved.

1. Introduction

Biological olfactory system has high sensitivity and specificity to discriminate different odors. As an excellent gas detecting system, the olfaction has become an interesting study object for its wide potential applications of environment monitoring, food safety, and medical diagnosis (Gilbert and Firestein, 2002). To achieve these goals, the electronic nose systems, which mimic the biological olfactory working process, are studied intensively. And, many achievements for gas detection have been made using absorbability or catalysis property of the sensing materials to special odors (Gopel et al., 1998; Rock et al., 2008). However, the electronic nose system is not so perfect as the biological olfaction in the performance of sensitivity and specificity, which mainly attribute to the well-evolved structure of the biological tissue and information coding mechanism.

The first stage of olfactory sensing occurs in the neurons of olfactory epithelium, where odorants interact with the olfactory receptors specifically, and chemical signal is converted into action potential of the neurons then electrical signal is delivered to the olfactory bulb to encode and decode, ultimately the smell information forms in the brain (i.e. Buck and Axel, 1991; Laurent, 1999; Narusuye et al., 2003; Liedo et al., 2005; Kleene, 2008). Nowadays, scientists have proposed the concept of bioelectronic nose to realize artificial olfaction biomimetic design (Gopel et al., 1998; Gopel, 2000; Minic-Vidic et al., 2006). Combining the biomolecular function units with sensors to construct the bioelectronic nose has become a new branch of olfactory biosensors. Using bioactive units directly, bioelectronic nose can promote the development of gas sensing, and establish a research platform for olfactory mechanisms.

In the recent research, cell and tissue based biosensors, which treat living cells as sensing elements, can collect the functional information of bioactive analytes (Bousse, 1996; Rudolph and Reasor, 2001; Wang and Liu, 2009). Neural cells and tissues can be extracted from primary sources and cultured *in vitro*. The electrical activities relating to cellular functions can be detected by microelectronic sensor chips. This novel biosensor technology, characterized with high sensitivity, excellent selectivity and rapid response, has been applied in environmental monitoring and biomedical diagnosing. In the previous study, we have tried to explore the cultured olfactory cells as sensing elements to fabricate the cell-based biosensor as a first step towards a neurochip of bioelectronic nose (Liu et al., 2006; Wu et al., 2009). The biosensor composed of light-addressable potentiometric sensor (LAPS)

* Corresponding author at: Biosensor National Special Laboratory, Key Laboratory of Biomedical Engineering of Education Ministry, Department of Biomedical Engineering, Zhejiang University, Zheda Road No. 38, Hangzhou 310027, Zhejiang, PR China. Tel.: +86 571 87952832; fax: +86 571 87951676.
E-mail address: cnpwang@zju.edu.cn (P. Wang).

0956-5663/$ – see front matter © 2010 Elsevier B.V. All rights reserved.
doi:10.1016/j.bios.2010.02.024

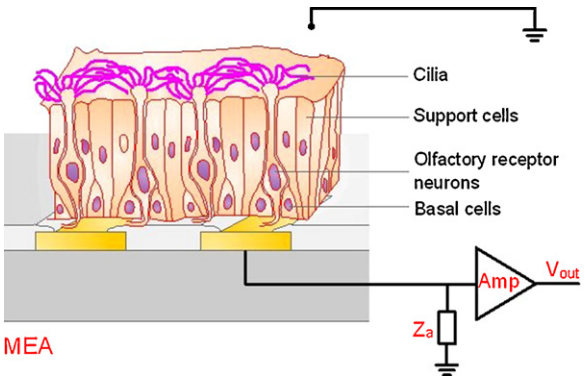

Fig. 1. Recording extracellular potentials of olfactory receptor neurons in intact epithelium by microelectrodes.

and olfactory neurons can monitor the extracellular potentials, and was sensitive to odorous changes. The most significant advantage is light addressable, which enables it to detect the potential changes on any site of the chip. However, the culture of olfactory cells on LAPS was relatively difficult. The living environment for cells changed from the original system. Besides, LAPS was a single channel recording system.

In contrast to LAPS, microelectrode array (MEA) can record the multisite potentials simultaneously and own the ability to long-term recording the firing of neural networks *in vitro* (Gross et al., 1995; Maher et al., 1999; Kovacs, 2003; Stett et al., 2003). In the present study, we managed to combine the intact olfactory epithelium with MEA for a bioelectronic nose of olfactory receptor neurons. Compared to the cultured olfactory cells, the intact olfactory epithelium can be obtained conveniently with the primary cell structure well preserved. Mimicking the *in vivo* process of gas sensing, it is a good candidate for the biological elements of bioelectronic nose. In our study, MEA can record the extracellular potentials of the olfactory receptor neurons in the epithelium. The multi-channel signal analysis might reveal some spatial and temporal information of early olfactory sensing for bioelectronic nose.

2. Theories

2.1. The structure and electrophysiology of the olfactory epithelium

In the olfactory epithelium, there are three types of cells: olfactory receptor neurons, support cells and basal cells (Fig. 1). The olfactory receptor neurons are sensory cells, which have axons and dendrites. Axons from neighboring receptor cells combine with each other, penetrate the basal membrane to form specialized nerve bundles and eventually connect to the brain. The cilia of these neurons, covered with olfactory receptors, are believed to be the odor's initial receptive field. Odor molecules interact with the olfactory receptor specifically, trigger the intracellular signal cascades and induce the action potential. The electric signal is finally transmitted to the brain. The support cells form the upper layer of the olfactory epithelium and connect to the basal membrane. The basal cells, which locate towards the basal side of olfactory epithelium, usually extend through the lower layer of the epithelium. Besides, there are a lot of glands to secrete the mucus, and the mucus layer forms humid environment to promote interaction between odorants and olfactory receptors.

Isolated neurons allow better control of the extracellular environment and odor delivery, however, the intact epithelium preserves native state of the neuron population and can be obtained easily (Reisert et al., 2005; Nickell et al., 2007). Olfactory neurons have different kinds of olfactory receptors and response to different odorants uniquely. The spatial and temporal coding is very important for olfactory systems. As a multi-channel recording device, MEA will greatly promote analyzing the coding information of the olfactory epithelium.

2.2. Theories of the tissue electrophysiological recording on MEA

MEA is a useful multi-channel recording device and has been extensively employed to record the tissue electrophysiological signals and study the spike firing mechanism. One successful example is spike recording in explanted retina by MEA (Grumet et al., 2000; Stett et al., 2003; Chen et al., 2003; Segev et al., 2004). By designing the electrode site area comparable in size to the ganglion cell, MEA can record from nearly all of the ganglion cells in a patch of the retina. This novel design provides a new way to understand neural circuits of retina *in vitro*.

In this paper, the intact olfactory epithelium was isolated and fixed on the surface of MEA. Fig. 1 illustrates the experiment of olfactory epithelium recorded by MEA. To record the electric signals from the epithelium efficiently, the basal membrane was contacted to the microelectrodes while the cilia were exposed. When the tissue is attached on the electrodes, a conductive cleft is formed between the tissue and the electrode, which is filled with electrolyte. A small patch of tissue is composed of many olfactory receptor neurons. Based on the H–H theory and the solid–electrolyte interface model, the transmembrane current of the cell–electrode junction is given by:

$$I_M = C_M \frac{dV_M}{dt} + I_{ionic} \quad (1)$$

where V_M is the transmembrane potential, C_M is the membrane capacitance per unit area, and I_{ionic} is the current due to ions flow through ion channels in the cellular membrane.

The I_{ionic} of the olfactory receptor neurons is defined as:

$$I_{total} = -(I_{CNG} + I_{ClCa} + I_{NCX}) \quad (2)$$

where I_{CNG} represents the inflow of Ca^{2+} and other extracellular cations through the cyclic nucleotide-gated (CNG) channels; I_{ClCa} represents the oulflow of Cl^- through Ca^{2+}-gated chloride (ClCa) channels; and I_{NCX} represents outflow of Ca^{2+} via the Na–Ca exchange protein.

The extracellular potential monitored by MEA is due to the ions flow through the cell membrane. The total field potential of the receptor neuron is given by:

$$\frac{V_i}{R_{seal}} + \frac{V_J}{Z_{electrode} + Z_a} = C_M \frac{d(V_M - V_J)}{dt} + I_{ionic} \quad (3)$$

where V_J is the polarization voltage detected by electrode. d is the thickness of average patch-to-insular distance. V_i is the transmembrane voltage. The transductive extracellular potential V_J represents general extracellular potential detected by MEA. R_{seal} is the seal resistance, which can be defined as:

$$R_{seal} = \frac{\rho_{seal}}{d} \frac{l}{w} \quad (4)$$

where ρ_{seal} is the sealing resistivity, l and w are the length and width of the effective portion of electrode coupled to the patch of the tissue, respectively.

Therefore, the microelectrodes with diameter of 30 μm were designed to record the extracellular potentials of olfactory receptor neurons. In order to get a successful recording of the potentials, "seal" impedance (voltage division of the signal) was decreased by electrodepositing platinum black onto the microelectrodes, and the thickness d was decreased by improving the adhesion of the tissue

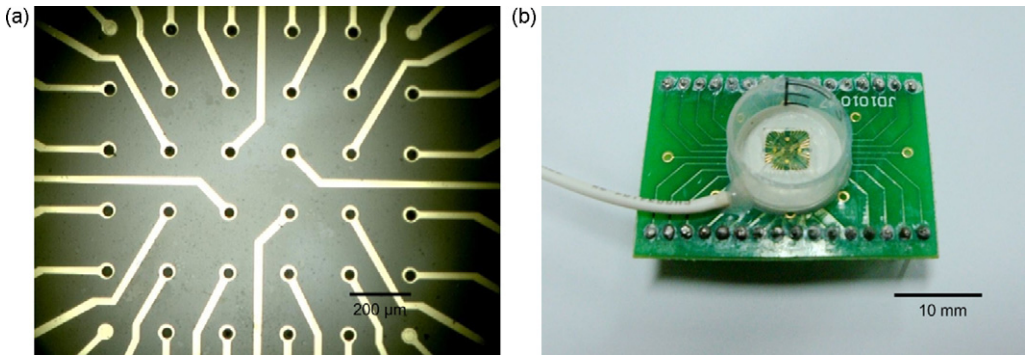

Fig. 2. Photos of the microelectrode array chip (A) and device (B).

to MEA. At last, the process of the odor stimulation was recorded by the microelectrodes.

3. Experimental and methods

3.1. Preparation of the microelectrode array

MEA is composed of an array of electrodes where intact olfactory epithelium was fixed for detecting electrophysiological properties of the receptor neurons, and the fabrication and preparation of MEA were similar to our previous work (Liu et al., 2009).

Firstly, a layer of Ti (30 nm) was deposited onto the glass substrate to enhance adhesion of the Au layer (300 nm). Then, the photoresist was spinning coated onto the metallic layer and exposed to ultraviolet light under the mask with defined electrode layout. As a result, the metal without protection by photoresist was removed while the electrodes and interconnects were formed. Subsequently, the Si_3N_4 layer (500 μm) for electric isolation of interconnects was deposited onto the chip by the process of PECVD (plasma enhanced chemical vapor deposition). Finally, the electrode array pattern and external contact pads were exposed etching by Si_3N_4 layer on them in 3–5% HF solution. The micrograph of the fabricated MEA with a 6×6 array pattern is shown in Fig. 2A. The electrodes were 30 μm in diameter with a 200 μm center to center spacing, which could avoid the electric interference between the neighboring electrodes effectively.

Leads from each electrode terminated at 36 separate pads on rectangular printed circuit board (PCB) shown in Fig. 2B, with 16 pads on each side to match the detecting system. The petri dish with diameter of 15 mm was fixed around the chip by epoxy and spiral platinum wire was used as the reference electrode.

Platinum black was electrodeposited onto exposed electrodes to improve the signal–noise-ratio of the chip (Ilic et al., 2000; Werdich et al., 2004), which was platinized at a constant voltage of 0.1 V for 25 s (EG&G Princeton Applied Research, M273A) by immersing electrodes in the petri dish solution medium (1% chloroplatinic and 0.01% acetate). Finally, a layer of "fluffy" platinum black was present on electrode. The impedance of electrodes was decreased by two orders at 1 kHz, and the noise was decreased to 15 ± 2 μV.

3.2. Isolation and fixation of olfactory epithelium

To improve the tissue adhesion, the sensor was initially covered with 3 ml dissolved cellulose nitrate (1 cm of Sartorius cellulose nitrate filter in 10 ml methanol) and dried in air (Chen et al., 2003). The coated cellulose nitrate film was cytocompatible, transparent, and sufficiently thin for the tissue-chip coupling.

Sprague–Dawley rats with weight of about 250 g were purchased from the Laboratory of Animal Research Center of Zhejiang Province, China. Rat was euthanized with intraperitoneal injections of Equithesine (mixture of pentobarbital sodium and chloral hydrate, 10 mL/kg). The head was hemisected in a midsagittal plane with the blade passing between the septum and the lateral wall. The olfactory epithelium covering the septum was removed from underlying cartilage and bone carefully (Nickell et al., 2007). The isolated epithelium (about 5 mm × 5 mm) was rinsed with Ringer's solution and placed with cilia receptors side up on the sensor surface. After rinsing, the solution was removed from the MEA petri dish and the tissue was fixed by a plastic ring-shaped frame covered with a tightly stretched piece of mesh.

The olfactory epithelium needed to sit for 5–8 min to make the tissue couple to the sensor tightly before odorant stimulations. The tissue was kept in standard perfusate containing (in mmol/L): 100 NaCl, 5 KCl, 3 $MgSO_4$, 1.8 $CaCl_2$, 25 $NaHCO_3$, 25 glucose, and bubbled with a mixed gas of 95% O_2 and 5% CO_2 with a pH of 7.5 ± 0.2.

The extended cilia, where the olfactory receptors located and specialized for odor detection, were observed by the scanning electron microscope (SEM). We found that olfactory cilia formed a dense meshwork on the olfactory epithelium. Therefore, the native cilia were very well preserved, with basic structures of receptor neuronal population intact.

3.3. Olfactory signals recording

We applied the USB-ME16-FAI system from Multichannel Systems (MCS, Reutlingen, Germany) for synchronously recording signals from 16 channels. The whole recording system was placed in the shielding box to avoid external electromagnetic interference. Noise level was maintained at about 20–40 μV peak-to-peak referred to the electrodes. The software MC_RACK was used to display and analyze the signals in real time with the gain of 1200 and the sampling rate of 20 kHz.

3.4. Odor stimulation and data processing

In our experiment, butanedione and acetic acid, as stimulus to the epithelium, were diluted in standard perfusate to 25 μmol/mL. Before odorant stimulation, epithelium activity was recorded for 5 min. After odorants being injected into the MEA chamber, the recording was lasted for about 5 min. Then the stimulus was washed out from the chamber by fresh standard perfusate. In order to rule out the influence of residual odorants and make electrodes and tissue return to a stable state, the minimum interval between the odor injections was 5 min. All solutions were added by a peristaltic pump and a selective valve. A computer was used to control the pump and the valves of flow system. All recordings were performed at 25 °C (room temperature). The signals recorded from multi-channels were analyzed by relevant signal processing methods.

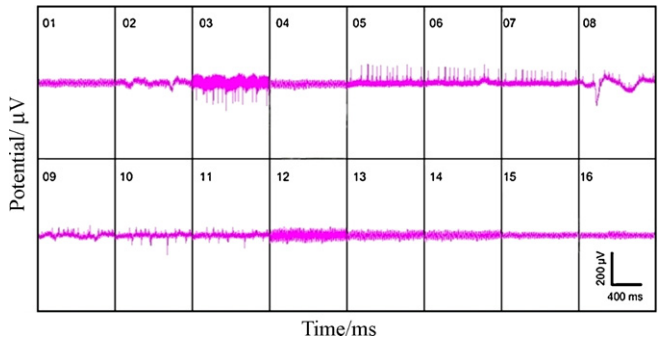

Fig. 3. Multi-channel recording electrophysiological signals of olfactory epithelium. The time is 1000 ms, and the amplitude is 1000 μV of each recording channel.

4. Results and discussion

4.1. Recording of electrophysiological signals

We designed a 36-channel MEA chip with the diameter of 30 μm to record the extracellular potentials simultaneously, making it easier to investigate synchronous activities of the cell networks. In olfactory epithelium, olfactory receptor neurons about 20 μm in diameter were among support cells and basal cells. The average size of isolated epithelium was about 5 mm × 5 mm in experiment. All the microelectrodes were covered by the tissue.

After olfactory epithelium was isolated and coupled to MEA, multi-channel spontaneous potentials can be detected. The *in vitro* tissue was kept bioactive, where olfactory receptor neurons fired spontaneously, with amplitude and duration of peaks about 50–100 μV and 10–20 ms, respectively. Fig. 3 displays the 16-channel signals as an example. It can be seen that Channel 03 recorded the negative peaks, while Channels 05, 06 and 07 recorded spontaneous potentials in cluster with similar positive peaks, whose average amplitude was larger than that in other channels. Channel 08 recorded small positive peaks with baseline drifting. Meanwhile, Channel 10 and Channel 11 recorded both positive and negative peaks with smaller amplitudes. Other channels had no obvious peaks only with steady baseline level at the moment, but there were peaks at other times.

The mechanism of spontaneous potentials is just like action potentials arising from odors in olfactory epithelium (Laurent, 1999; Dougherty et al., 2005). It triggers the opening of cyclic nucleotide-gated (CNG) channels, allowing calcium and other extracellular cations into the cilia and generates an inward current. Elevated Ca^{2+} levels in the cilia activate Ca^{2+}-gated chloride [Cl(Ca)] channels, creating an outflow of Cl^- ions and thus increase the inward current, which results in membrane depolarization and the generation of action potentials in the olfactory receptor neurons. Based on theories of the tissue recording on MEA, the transmembrane potential was finally recorded as transductive extracellular potentials, which is due to the reduction of electrode seal impedance and the improvement of tissue adhesion in the experiment.

4.2. Analysis of multi-channel signals

MEA has the benefit of detecting signals of many cells synchronously, which is convenient to comparatively analyze recorded information in parallel. Several experiments based on the *in vitro* neurons coupling to MEA suggested that synchronism of activities in neuron networks was considered as one of the elementary features (Chen et al., 2003; Selinger et al., 2004; Eytan et al., 2004; Chiappalone et al., 2006). To investigate whether the main feature was preserved in our olfactory tissue, we tracked the tissue behavior by computing the cross-correlation coefficients of the spike chains recorded by MEA.

We extracted a segment of data with the length of 10 s from different channels for cross-correlation calculation, which was defined as:

$$r_{XY} = \frac{C_{XY}}{\sigma_X \sigma_Y} \tag{5}$$

$$C_{XY} = E[(X - E[X])(Y - E[Y])] \tag{6}$$

where X and Y are data with the length of N ($N > 1$), r_{XY} is the cross-correlation coefficient; C_{XY} represents the covariance of X and Y; σ_X and σ_Y are the standard deviation of X and Y, respectively, while $E[X]$ and $E[Y]$ represent the mean values.

Fig. 4 shows the cross-correlograms of the signals obtained from active electrodes in Fig. 3. Channel 05 and Channel 11 were selected as the different centers to calculate cross-correlations with all of the other active channels. The maximum absolute cross-correlation coefficient of Channel 05 and the neighboring channels was larger than 0.5, but the coefficients of Channel 05 to Channel 07 and Channel 05 to Channel 11 were only 0.31 and 0.28, respectively, in Fig. 4A. Meanwhile, cross-correlation was analyzed between Channel 11 and the other channels as shown in Fig. 4B. Coefficient of Channel 11 to Channel 10 was 0.73. As the channels were farther away from Channel 11, the coefficients became smaller. In the case, the autocorrelation was included as well, and the coefficient was 1. Consequently, from the comparison of correlations in these different active channels, the recorded spikes can be sorted into two different kinds. One focused in Channels 03, 05, 06, 07, 08 and 09, and the other focused in Channels 10 and 11.

Previous studies of correlation of cultured neuron networks on MEA, have found that the homogeneous chains of subpopulations were connected by synapse with spatially neighboring sites (Eytan et al., 2004; Chiappalone et al., 2006). However, olfactory receptor neurons never connect with each other by synapse in epithelium, only with the support cells regulating the interstitial compartments. Although olfactory potentials primarily arise from the receptor neurons, support cells are also possible to contribute to the potentials directly (Reisert et al., 2005; Nickell et al., 2007). And, olfactory receptors are classified into different groups, according to their expression patterns in the epithelium (Laurent, 1999; Mori et al., 1999). Receptor position is an intrinsic component of the olfactory encoding. Such spatial code is the initial step for understanding the functional roles of sensory neurons in the epithelium. In this study, we also presented evidence of changes arising in isolated olfactory epithelium tissue and correlations between all the possible pairs of active channels, demonstrating the spatio-temporal pattern of firing in the tissue during the *in vitro* recording.

Therefore, multi-channel recording systems allow monitoring activities at many sites simultaneously in olfactory epithelium tissue. This capability was utilized to record correlated spontaneous firing, which suggested the anatomical substrates underlying different spike patterns. At the same time, the correlation pattern analysis of neighboring channels provides more information about the neural activity during various experimental conditions.

4.3. Odor detection and analysis

Studies by SEM have found that the functional units of the cilia on the cell membrane were well preserved in the tissue on MEA. In our previous studies, primary cultured olfactory cells can be stimulated by the odorants of acetic acid (CH_3COOH, an organic acid, with a distinctive pungent odor) (Liu et al., 2006). Therefore, it was used as a stimulus of olfactory receptor cells to inspect the sensitivity of MEA in our study. Besides, butane-

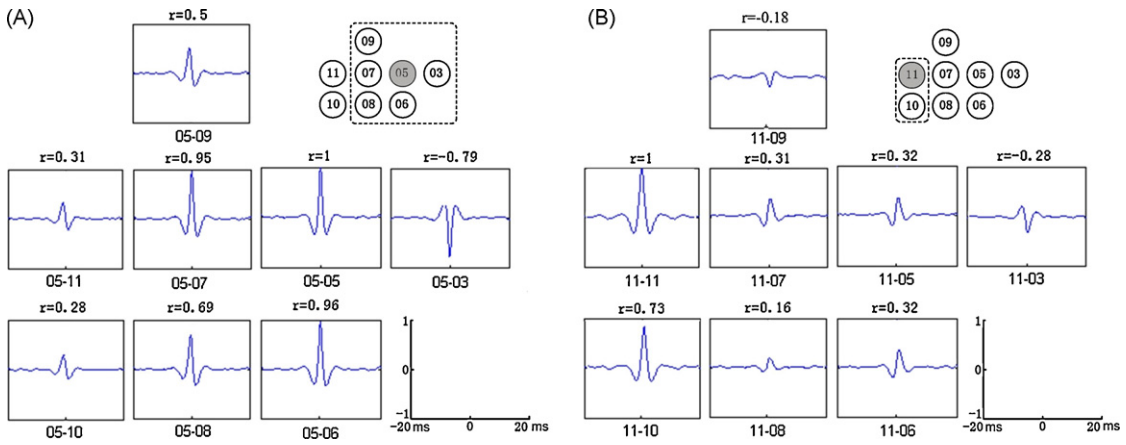

Fig. 4. Cross-correlations of olfactory epithelium signals recorded by microelectrode arrays. (A) The analysis of 05 Channel to other active channels; (B) the analysis of Channel 11 to other active channels. The autocorrelation is also calculated, and it corresponds to the maximum value. Each correlation coefficient is denoted with *r*. The distribution of electrodes is illuminated on the top right corner, with dotted box partitioned different functional units of the signals. The standard axes of −20 ms to 20 ms to the cross-correlograms are illuminated on the right bottom corner.

dione ($CH_3CO–COCH_3$, a natural byproduct of fermentation, occurs naturally in alcoholic beverages and is added to some food to impart a buttery flavor) was used as another stimulus for comparison.

On the basis of effectively recording spontaneous potentials, we recorded electrophysiological signals after odor stimulations. Fig. 5 shows the stimulated potentials compared with spontaneous potentials in one of the channels on MEA. Spontaneous potentials fired every second. The release of potentials after acetic acid stimulation was mainly about sustained signals with significant amplitudes in a short time, while the release of potentials after butanedione stimulation was mainly about long-term signals with low amplitudes. The frequency and amplitude of the olfactory epithelium potential changed with stimulation of different odors, showing some characteristics of the discharge modes.

Power spectrum analysis of olfactory cells response to odors was often used to calculate the distribution of frequency band during odor presentation (Lowry and Kay, 2007; Ito et al., 2006). In order to discuss whether there were different firing modes during the odors detection and recognition, we analyzed the power spectrum of signals in Fig. 6. When olfactory epithelium tissue was immersed in standard perfusate, there was only one obvious peak in low-frequency part of the power spectrum, while there were several obvious peaks after stimulation of odors. Under the stimulation of acetic acid, three obvious peaks of power spectrum were at the frequency of 6.8 Hz, 8.7 Hz, and 11.2 Hz, while the obvious peaks located at the frequency of 5.8 Hz, 7.0 Hz, and 8.5 Hz under the stimulation of butanedione. The specific peaks in the power spectrum may indicate the periodic activities in olfactory system. The power spectrum was significantly higher in response to different odorants due to signal enhancement after stimulation

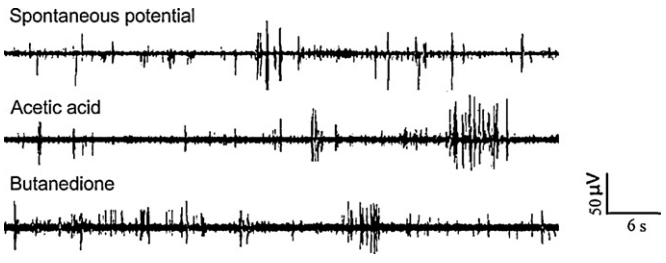

Fig. 5. Changes of electrophysiological signals after the stimulation of acetic acid and butanedione.

Recently, some groups have tried to fabricate the gas biosensor by using the biological components, such as insect antenna and human embryonic kidney-293 cells to obtain high specificity and sensitivity to odors (Schutz et al., 2000; Hwi and Tai, 2005; Ko and Park, 2005; Sung et al., 2006; Lee et al., 2006). However, the tissue or cells they employed were not olfactory receptor neurons, and the parameters detected by those sensors were also not the neurons potentials. In vertebrates, the olfactory events are triggered by the bioelectrical signals of the olfactory receptor neurons after the binding of odorant molecules to the receptors. Therefore, if olfactory neurons are employed as sensitive materials to develop a bioelectronic nose, the bionic design will have high performance in odor detection. The olfactory epithelium is a natural nervous tissue "slice" that can be easily exposed, dissected, and manipulated without damaging its functional integrity. The defined epithelial strata afford facile identification of extracellular electrophysiological recording sites with microelectrodes. In the study, we can distinguish the different discharge modes of spontaneous signals from those after the stimulation of butanedione and acetic acid both in time and in frequency domain. The differences of spatio-temporal analysis may provide powerful support with pat-

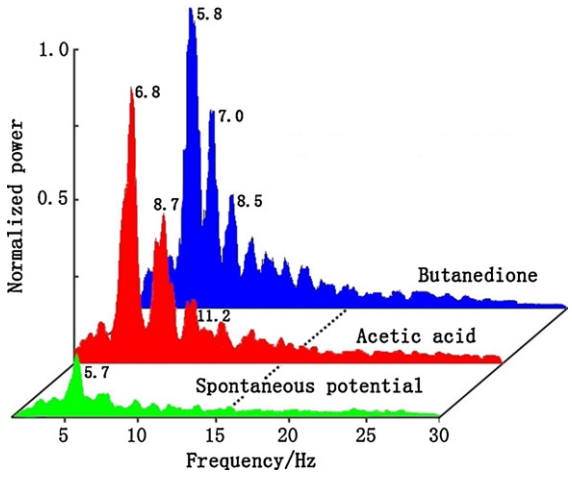

Fig. 6. Power spectrum analysis of the signals. The green represents the power spectrum of spontaneous signals, and the red and the blue represent the power spectrum of signals obtained after stimulation of acetic acid and butanedione, respectively. The difference of the frequency is labeled to those obvious peaks of power spectrum. (For interpretation of the references to color in this figure legend, the reader is referred to the web version of this article.)

tern recognition for a practical bioelectronic nose system in the future.

5. Conclusions

Combining biological olfactory tissue with micro-chip technology, this study tried to design a novel bioelectronic nose for odor detection by electrophysiological sensing measurements of olfactory receptor neurons in their native environment in the organic level. Extracellular potentials of olfactory receptor neurons in intact olfactory epithelium were recorded through multi-channel MEA recording systems. The firing potentials were effectively analyzed by correlation analysis between different channels. When stimulated by odors, the recorded potentials represented different firing modes and contributed to obvious characters of power spectrum analysis. With natural neuronal populations well preserved and successfully recorded, the receptor cell-based biosensor technology is a promising platform for bioelectronic nose with respect to odors detection in the intact cellular environment of the olfactory epithelium.

Acknowledgments

This work was supported by the National Natural Science Foundation of China (Grant Nos. 30700167 and 60725102), the Project of State Key Laboratory of Transducer Technology of China (Grant No. SKT0702), and the Zhejiang Provincial Natural Science Foundation of China (Grant No. Y2080673).

References

Bousse, L., 1996. Sens. Actuators B 34, 270–275.
Buck, L., Axel, R., 1991. Cell 65, 175–187.
Chen, A., Zhou, Y., Gong, H., Liang, P., 2003. Sci. China Ser. C 46, 414–421.
Chiappalone, M., Bove, M., Vato, A., Tedesco, M., Martinoia, S., 2006. Brain Res. 1093, 41–53.
Dougherty, D.P., Wright, G.A., Yew, A.C., 2005. Proc. Natl. Acad. Sci. U.S.A. 102, 10415–10420.
Eytan, D., Minerbi, A., Ziv, N., Marom, S., 2004. J. Neurophysiol. 92, 1817–1824.
Gilbert, A.N., Firestein, S., 2002. Nat. Neurosci. 5, 1043–1045.
Gopel, W., Ziegler, C., Breer, H., Schild, D., Apfelbach, R., Joerges, J., Malaka, R., 1998. Biosens. Bioelectron. 13, 479–493.
Gopel, W., 2000. Sens. Actuators B 65, 70–72.
Gross, G.W., Rhoades, B.K., Azzazy, H.M., Wu, M.C., 1995. Biosens. Bioelectron. 10, 553–567.
Grumet, A.E., Wyatt Jr., J.L., Rizzo, J.F., 2000. J. Neurosci. Methods 101, 31–42.
Hwi, J.K., Tai, H.P., 2005. Biosens. Bioelectron. 20, 1327–1332.
Ilic, B., Czaplewski, D., Neuzil, P., Stanczyk, T., Blough, J., Maclay, G.J., 2000. J. Mater. Sci. 35, 3447–3457.
Ito, I., Watanabe, S., Kirino, Y., 2006. J. Neurophysiol. 96, 1939–1948.
Kleene, S.J., 2008. Chem. Senses 3, 839–859.
Ko, H.J., Park, T.H., 2005. Biosens. Bioelectron. 20, 1327–1332.
Kovacs, G.T.A., 2003. Proc. IEEE 91, 915–929.
Laurent, C., 1999. Science 286, 723–728.
Lee, J.Y., Ko, H.J., Lee, H.S., Park, T.H., 2006. Enzyme Microb. Technol. 239, 375–380.
Liedo, P.M., Gheusi, G., Vincent, J.D., 2005. Physiol. Rev. 85, 281–317.
Liu, Q., Cai, H., Xu, Y., Li, Y., Li, R., Wang, P., 2006. Biosens. Bioelectron. 22, 318–322.
Liu, Q., Yu, J., Xiao, L., Tang, J.C.O., Zhang, Y., Wang, P., Yang, M., 2009. Biosens. Bioelectron. 24, 1305–1310.
Lowry, C.A., Kay, L.M., 2007. J. Neurophysiol. 98, 394–404.
Maher, M.P., Pine, J., Wright, J., Tai, Y.C., 1999. J. Neurosci. Methods 87, 45–56.
Minic-Vidic, J., Grosclaude, J., Persuy, M.A., Aioun, J., Salesse, R., Pajot-Augy, E., 2006. Lab Chip 6, 1026–1032.
Mori, K., Nagao, H., Yoshihara, Y., 1999. Science 286, 711–715.
Narusuye, K., Kawai, F., Miyachi, E., 2003. Neurosci. Res. 46, 407–413.
Nickell, W.T., Kleene, N.K., Kleene, S.J., 2007. J. Physiol. 583, 1005–1020.
Reisert, J., Lai, J., Yau, K.-W., Bradley, J., 2005. Neuron 45, 553–561.
Rock, F., Barsan, N., Weimar, U., 2008. Chem. Rev. 108, 705–725.
Rudolph, A.S., Reasor, J., 2001. Biosens. Bioelectron. 16, 429–431.
Schutz, S., Schoning, M.J., Schroth, P., Malkoc, U., Weibecker, B., Kordos, P., Luth, H., Hummel, H.E., 2000. Sens. Actuators B 65, 291–295.
Segev, R., Goodhouse, J., Puchalla, J., Berry, M.J., 2004. Nat. Neurosci. 7, 1155–1162.
Selinger, J.V., Pancrazio, J.J., Gross, G.W., 2004. Biosens. Bioelectron. 19, 675–683.
Stett, A., Egert, U., Guenther, E., Hofmann, F., Meyer, T., Nisch, W., Haemmerle, H., 2003. Anal. Bioanal. Chem. 377, 486–495.
Sung, J.H., Ko, H.J., Park, T.H., 2006. Biosens. Bioelectron. 21, 1981–1986.
Wang, P., Liu, Q., 2009. Cell-based Biosensors: Principles and Applications. Artech House Publishers, USA.
Werdich, A.A., Lima, E.A., Ivanov, B., Ges, I., Anderson, M.E., Wikswo, J.P., Baudenbacher, F.J., 2004. Lab Chip 4, 357–362.
Wu, C., Chen, P., Yu, H., Liu, Q., Zong, X., Cai, H., Wang, P., 2009. Biosens. Bioelectron. 24, 1498–1502.